



Control of Protrusion Induced Unsteady Supersonic Separation Using Boundary Layer Suction

Hemanth Chandra Vamsi Kakumani, Sourabh Bhardwaj and
Sriram Rengarajan

EasyChair preprints are intended for rapid
dissemination of research results and are
integrated with the rest of EasyChair.

November 4, 2020



CONTROL OF PROTRUSION INDUCED UNSTEADY SUPERSONIC SEPARATION USING BOUNDARY LAYER SUCTION

Hemanth Chandra Vamsi K, S. Bhardwaj, R. Sriram

Indian Institute of Technology Madras, Chennai, 600036, India

ae18m037@smail.iitm.ac.in

Abstract The unsteady 3-dimensional separated flow induced by a square protrusion (measuring twice the local boundary layer thickness in both its width and height denoted by h), and its control by means of boundary layer suction through holes, is investigated using wind tunnel experiments and computations. Surface oil flow visualization, time resolved schlieren using high speed camera and surface static pressure measurements using pressure scanner are the diagnostics used to study the 3-dimensional shock boundary layer interaction. Unsteady-RANS computations are validated using the experimental data, and are used to complement the understanding of the flow field. It was observed from the oil-flow visualizations that at the span-wise centre, the separation location was at $2.6h$ from the protrusion. The time averaged foot of the separation shock measured from the schlieren images was at $2.80h$ from the protrusion. The computational results compared well with the visualizations as well as the surface pressure data. The computation of flow field with suction through holes upstream of protrusion suggested the emergence of interesting 3-dimensional flow patterns.

1 Introduction

Local unsteady thermo-mechanical loading over a surface due to Shock-wave boundary layer interaction (SBLI) is a common ramification in many high speed applications where shock formed because of various reasons (obstacle, presence of corner, shock due to off-design conditions etc.) interacts with the local laminar/turbulent boundary layer. Due to the advancements in diagnostics and computations, the low-frequency unsteadiness in turbulent SBLI due to nominally 2-dimensional geometric configurations has been resolved in recent times [1]. The nature of 3-dimensional SBLI is still under early exploration stages and few recent advancements [2, 3, 4] in this field have addressed the shock structures and separation geometries using various configurations under different flow parameters. Various flow control techniques for unsteady SBLI have been explored and demonstrated successfully for nominally 2-dimensional configurations [5, 6]. The objective of this research is to understand the nature of protrusion induced unsteady separated flow field, and explore the possibility of controlling the flow field by means of boundary layer suction.

2 Set-up for Experimental and CFD Analysis

2.1 Experimental Set-up

Experiments were performed at nominal Mach number of 3, in the supersonic blowdown wind tunnel at the Gas Dynamics Laboratory, IIT Madras. The tunnel is being operated

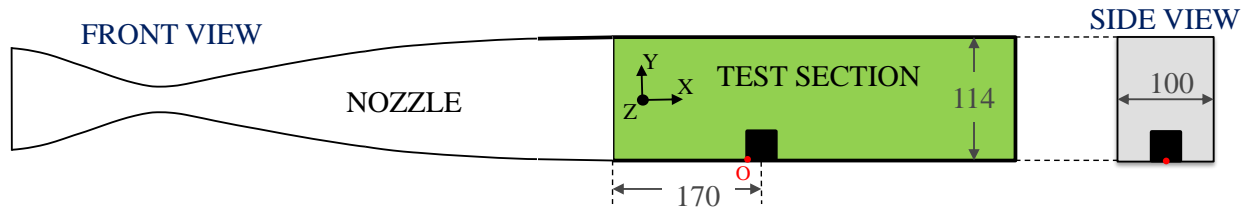


Fig.1 Schematic drawing of nozzle and test section assembly (with dimensions in mm)

at a nominal stagnation pressure P_o of 5.5 bar (absolute) with each run lasting less than 10 seconds. Schematic of the wind tunnel, including the nozzle, test section and protrusion is shown in Fig.1. Using pitot survey the boundary layer thickness ($\delta_{99\%}$) at 170 mm from the nozzle end was found to be 7 mm. The protrusion was thus chosen to be 15 mm in height and width, which is around twice the local boundary layer thickness. Freestream conditions estimated from wall static pressure and stagnation pressure at core of the test section are summarised in the table at the end of this section.

Time resolved schlieren visualizations were taken at 30,000 fps for a qualitative understanding of the flow field and shock-foot unsteadiness for baseline and control cases. Surface oil flow streak-line visualisation technique was used to identify important regions in the flow field, and this information shall be used for the placement of bleed holes as well as the placement of pressure ports. A set of discrete suction vents in different configurations will be introduced on the bottom wall (based on computational results and experimental observations) as a strategy to overcome unsteadiness. Data obtained from pressure transducers and schlieren images will be used to assess the extent of control qualitatively and quantitatively in future.

2.2 Computational Set-up

Computations have been performed using the open-source toolbox OpenFOAM-v1906. The solver employs PISO algorithm to solve unsteady-compressible forms of continuity equation, Reynolds-averaged Navier–Stokes equations and energy conservation equation along with Menter’s k- Ω SST turbulence model as closure. All the computations have been carried out in Virgo super cluster at HPCE, IIT Madras.

The computational flow domain was taken to be a segment of the experimental flow-domain which encompasses protrusion along with sufficient upstream and downstream flow volume which allowed us to study separation bubble and the shock topology. A structured mesh with roughly twenty lakh nodes was constructed and the near wall mesh resolution was taken care to ensure y^+ values close to 1. While the bottom wall was enforced with adiabatic no-slip boundary condition and the top-wall with adiabatic free-slip condition, the side planes were set to follow symmetry boundary condition. Furthermore in order to provide proper inflow condition (consisting of free stream and boundary layer profile) the inlet was mapped with field values which were generated from another flow simulation in the geometry that was replica of experimental set-up consisting of nozzle and an empty test-section carried out using the same solver. The validity of this inflow was checked experimentally by free-stream and boundary layer survey (at 170 mm away from the nozzle exit). The computational results for free-stream are also summarised in

the table at the end of this section. The outflow was provided with wave-transmissive pressure outlet (standard atmospheric pressure) condition.

Based on the preliminary computational and experimental analysis of “baseline case”, the “control cases” were set-up. The first configuration of bleed-vents was carried out with one hole at the span-wise centre-line and the second simulation was done with three serially placed holes along the span-wise centre-line (maintaining a constant gap of $0.84h$ between holes) with one at mean separation position and two inside separation bubble. The bleed vents were enforced with wave-transmissive pressure outlet boundary condition which sucks the fluid stream down with a vacuum pressure of 5 kPa.

	δ	M	Re	U	P	T	P_o
Experiment	7 mm	2.87	$40.4 \times 10^6 / m$	612 m/s	22063 Pa	114 K	5.5 bar
RANS	6.5 mm	2.92	$40.7 \times 10^6 / m$	617 m/s	18478 Pa	110 K	5.5 bar

3 Results and Discussion

An array of 30 static pressure ports were mounted on the bottom surface of the test-section at the locations shown in the following plot (Fig.2), to extract and compare the static pressure values with that of the computations. All the computational pressure values and experimental pressure values have been normalised with their respective free-stream values and the percentage difference between them was calculated (represented in the figure with red font). The small differences between experimental and computational data confirms the reliability of the RANS simulations.

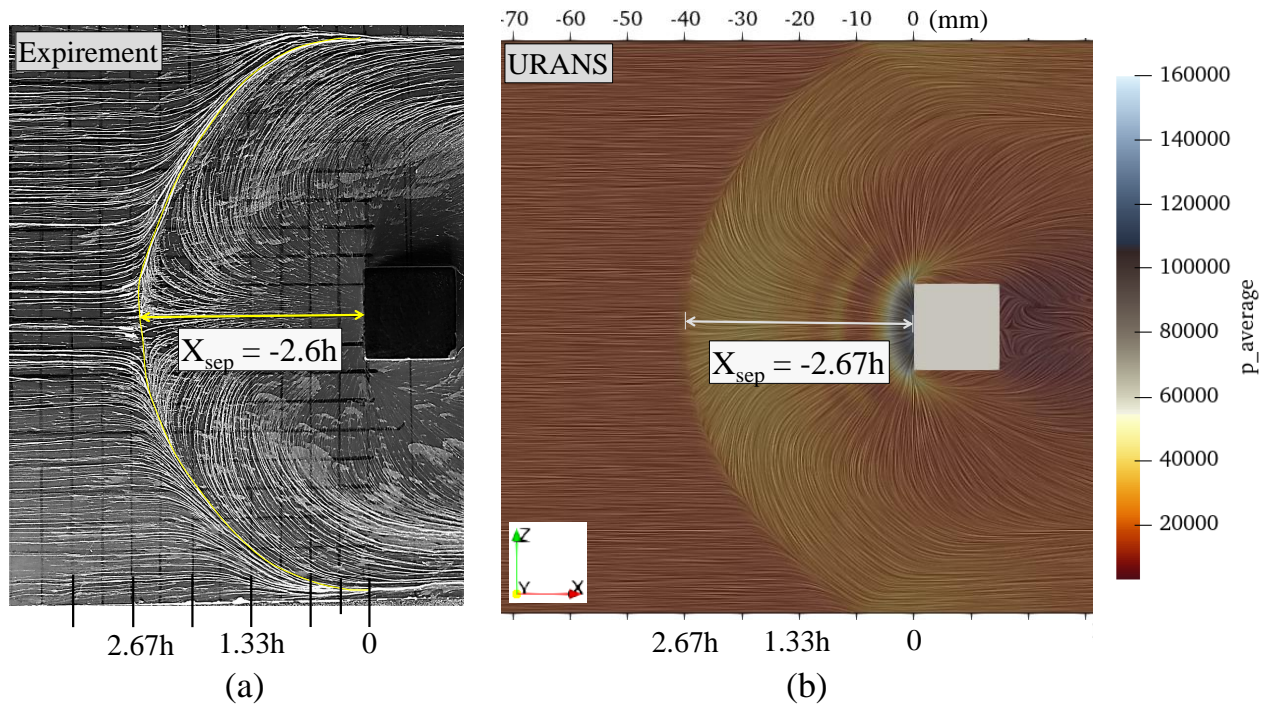


Fig.3 Comparison of experimental and computational (RANS) streak line patterns on protrusion mounted wall.

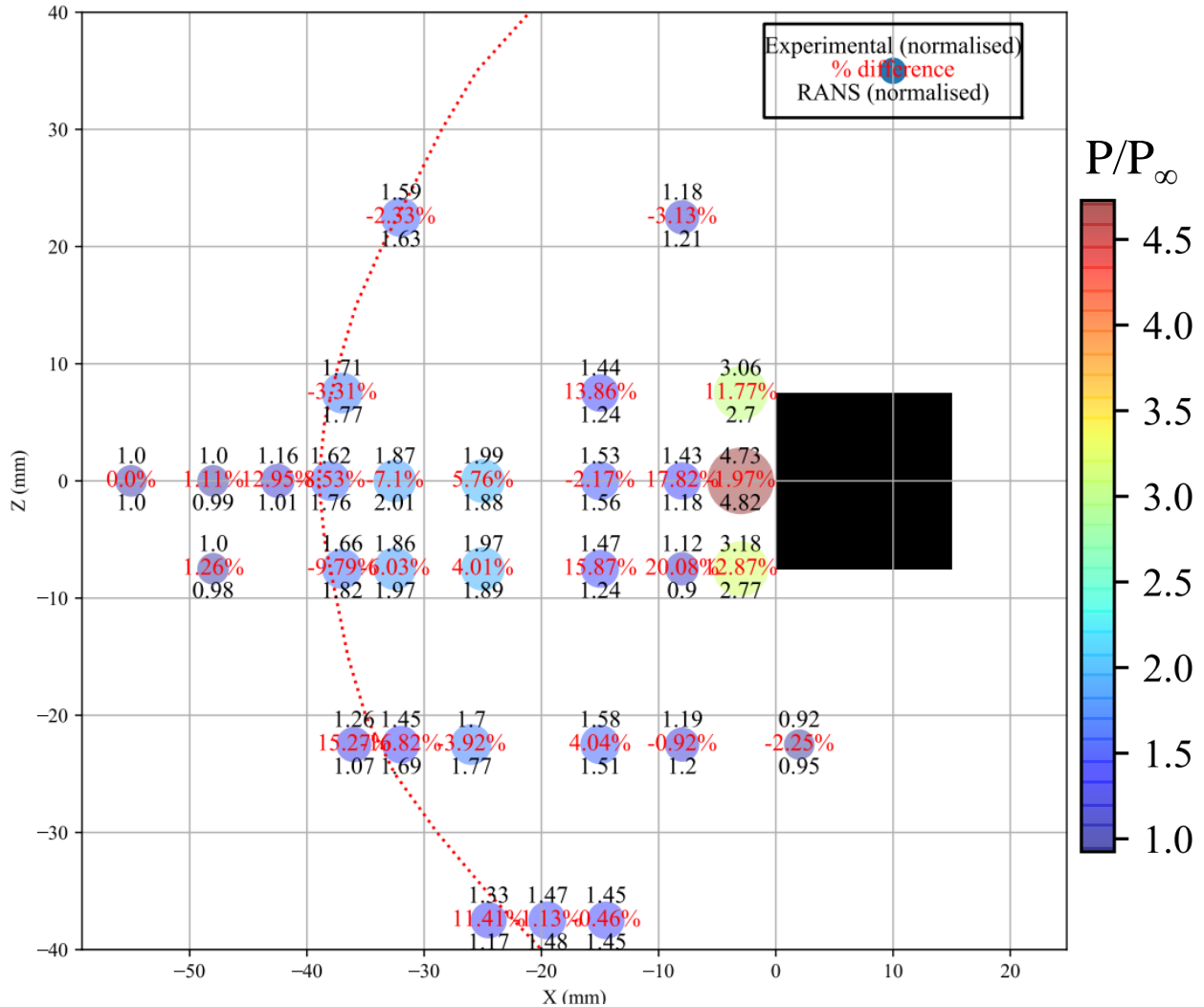


Fig.2 Comparison of experimental (mentioned on the top of solid circle) and computational (mentioned below the solid circle) static pressure values on the bottom surface of the test section. (the dotted line represents downstream location of separation shock foot which was extracted from oil-flow data)

Oil-flow visualisation had revealed the streak line pattern and separation line geometry on the bottom wall as shown in the Fig.3. Surface streak lines obtained through RANS simulations compare well with experiments.

The 3-dimensional lambda shock structure observed from the schlieren photography and from the numerical schlieren from RANS simulations (as shown in the Fig.4 (a), (b)) compare well. Three thousand schlieren snapshots were taken, and standard deviation of intensity values at each pixel for all the snapshots was calculated, whose map is shown in the Fig.4 (c). The result indicates that the shock sweeping length ($= 1.14\delta$) was comparable to the thickness of the incoming boundary layer.

Preliminary unsteady-RANS computations with bleed were done to get an idea of the effect and performance of bleed holes on the separation shock geometry and the flow field around it. The simulations suggest that the addition of these holes induces span-

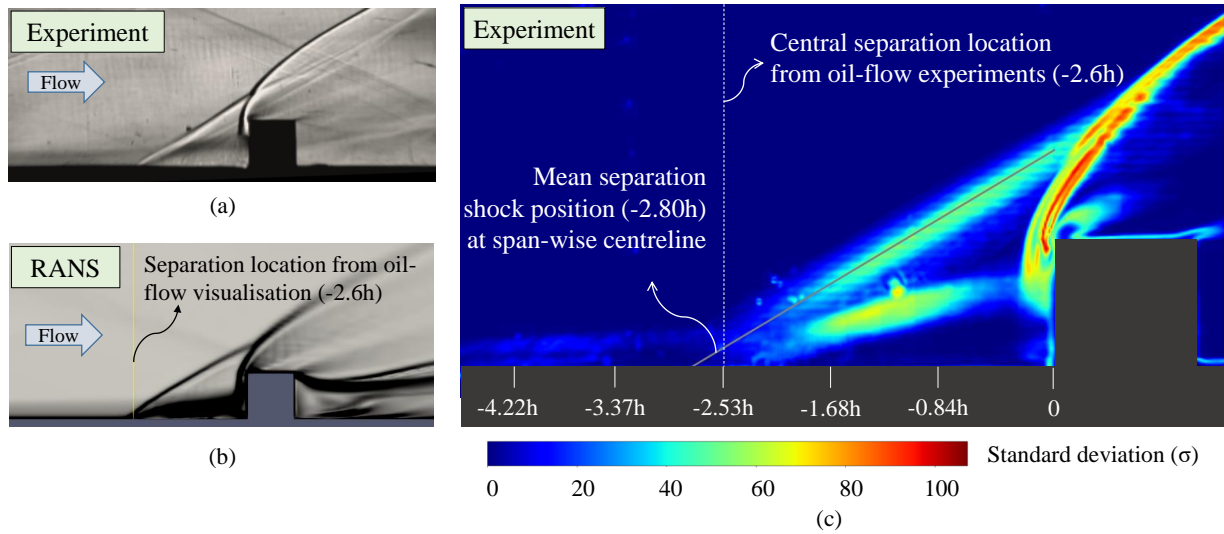


Fig.4 (a) Experimental schlieren (b) Computational schlieren (at span-wise central plane) (c) A picture generated by taking standard deviation at each pixel from 3,000 time resolved schlieren snap shots taken at 30,000 fps.

wise unsteady motion of separation shock foot. Though the hole added at the separation shock foot has not affected the geometry of separation shock much, the overall separation bubble size/separation length was observed to decrease. The bleed holes placed inside the separation bubble (in 3-bleed holes case) seem to have a clear anchoring/pulling effect on the separation shock which has reduced the separation length and unsteadiness locally to a considerable amount. Apart from the central portion (in bleed 3-holes case) of the separation the average span-wise positioning of the separation shock has also been observed to shift downstream. We speculate that adding more bleed holes in the span-wise direction may improve the overall control effect by obstructing the shock motion and decreasing the separation bubble size. Experiments are underway with bleed holes.

4 Conclusion and future scope

The base-line experiments with supersonic flow ($M = 2.87$) over square protrusion, roughly twice the local boundary layer thickness in width and height (h), revealed λ -shock structure and 3-D separation bubble in-front of the protrusion. From the time resolved schlieren observations, the shock-foot was at $2.80h$ from protrusion on an average, and had a sweep length (1.14δ) comparable to boundary layer thickness. Mean separation line was identified using surface oil flow visualization; the separation at spanwise center was identified to be $2.6h$ from protrusion. Through essential validation from the experiments, RANS simulations were also used to understand features such as shock structure, mean separation bubble location/size and pressure distribution around protrusion. Although the solver failed to resolve the unsteady characteristics, the mean flow field (in no-control case) matches very well with the experiments. While control experiments are still underway, the computations with bleed through holes along the span-wise centre-line has revealed that suction vents placed inside the separation bubble affects the size, shape

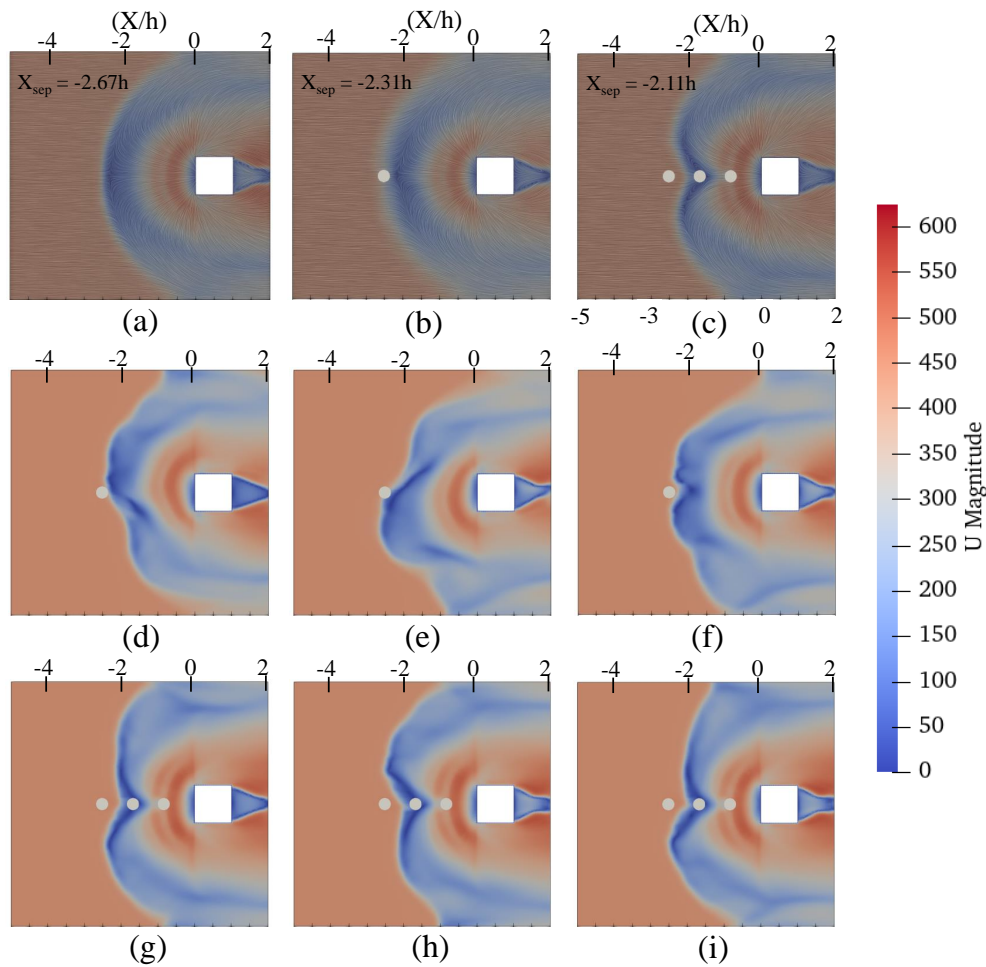


Fig.5 (Note: Horizontal-axis scale is plotted in the units of h) **(a,b,c)** Comparison of shock separation patterns between base-line **(a)** and control cases **(b, c)** with the average velocity data extracted from the cut-planes 0.5 mm above the bottom surface. **(d,e,f)** Instantaneous snapshots taken from simulation with 1-bleed hole (bleed hole placed at $-2.52h$ away from protrusion). **(g,h,i)** Instantaneous snapshots took from simulation with 3-bleed holes (bleed holes were placed at $-2.52h$, $-1.68h$ and $-0.84h$ away from protrusion).

and unsteadiness/motion of the separation bubble. The insights from these investigations shall be used to further understand and devise control strategy for shock induced 3-D separation. Experiments are underway using fast response pressure sensors to study the space-time correlation in the flow field with and without bleed.

References

- [1] Noel T. Clemens and Venkateswaran Narayanaswamy, Low-Frequency Unsteadiness of Shock Wave/Turbulent Boundary Layer Interactions, 46, 2014
- [2] S. Mowatt and B. Skews, Three dimensional shock wave/boundary layer interactions, Shock Waves, 21, 2011.
- [3] S. Bhardwaj and R. Sriram, Unsteadiness in Shock Induced Separation due to Protrusions, International Symposium on Shock Waves -32, Singapore 2019.



6th National Symposium on Shock Waves - IITM (NSSW-2020)

- [4] J.D. Pickles, B.R. Mettu, P.K. Subbareddy and V. Narayanaswamy, On the mean structure of sharp-fin-induced shock wave/turbulent boundary layer interactions over a cylindrical surface, *J Fluid Mechanics*, 865, 2019.
- [5] R. Sriram and G. Jagadeesh, Shock tunnel experiments on control of shock induced large separation bubble using boundary layer bleed, *Aerospace Science and Technology*, 36, 2014.
- [6] S.B. Verma and C. Manisankar, Shockwave/Boundary-Layer Interaction control on a Compression Ramp Using Steady Microjets, *AIAA Journal*, 50, 22, 2012.